Unraveling the hydrocracking capabilities of fluidized bed systems operated with natural ores as bed materials

Journal of Analytical and Applied Pyrolysis 166 (2022) 105603

Contents lists available at ScienceDirect

Journal of Analytical and Applied Pyrolysis

journal homepage: www.elsevier.com/locate/jaap

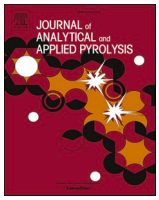

Unraveling the hydrocracking capabilities of fluidized bed systems operated with natural ores as bed materials

Chahat Mandviwala *, Teresa Vilches Berdugo, Martin Seemann, Judith González-Arias, Henrik Thunman

Department of Space, Earth and Environment (SEE), Division of Energy Technology, Chalmers University of Technology, 412 96 Gothenburg, Sweden

ARTICLE INFO

Keywords:
Plastic waste
Polyethylene
Hydrocracking
Fluidized bed
Water dissociation
Hydrogen donation

ABSTRACT

Hydrocracking represents an alternative to the recycling of abundantly available plastic waste. Hydrocracking of polyethylene in a fluidized bed, at 750 °C and 1 atm, was investigated in this work. Water dissociation, through the steam-iron reaction, was used as the source of hydrogen. Bauxite and olivine, containing reduced iron, were used as the bed materials in the reactor to drive the water dissociation reaction. The hydrogen-to-carbon (H/C) ratios of the products were compared to assess the hydrocracking potential. It was discovered that conversion of polyethylene on the surface of reduced bauxite effectively increased the H/C ratios of the products, as compared to bauxite in its oxidized form. Reduced olivine was ineffective at increasing the H/C ratios of the products in the presence of water dissociation. It is concluded that hydrocracking through hydrogen donation by steam is feasible in fluidized beds, provided that the bed material has the ability to transfer the hydrogen atoms to the hydrocarbon species.

1. Introduction

Sustainable production and eventual disposal of plastic materials are serious problems faced by humanity in this century. Almost 99% of the plastic materials in use today are derived from fossil-based carbon reserves [1]. In addition, the lifecycle of plastic materials remains linear to a large extent. Only 9% of all the plastic materials produced in Year 2019 were recycled, with 19% being incinerated, 49% being dumped in landfills, and 22% being mismanaged or littered in the environment [2]. The current production and waste-handling strategies make the production of plastic materials based on fossil reserves unsustainable. Substitution of fossil reserves with reusable and recycled resources for the production of plastic materials is, therefore, essential.

Progress towards a fossil-independent plastic economy requires the implementation of a technology that enables 100% circular use of any plastic material. Thermochemical recycling is one such approach that allows limitless recycling of any plastic material, where the prime focus is on the recovery of chemicals that can be used for the production of new plastic materials [3]. Thermochemical recycling forms a bridge between the production of new plastic materials and waste handling of used plastic materials, thereby closing the material cycle.

In the past, different reactor set-ups and techniques have been investigated for thermochemical recycling of plastic materials for the production of useful chemicals [3–6]. Fluidized bed reactors are, in this case, deemed suitable for thermochemical recycling of plastics due to their heat transfer properties and ability to treat heterogeneous feedstocks [3–5]. Kaminsky et al. investigated fluidized bed pyrolysis of mixed plastic waste for the production of monomers for polymer synthesis and obtained a product distribution rich in light olefins and mono aromatics [5]. Thunman et al. demonstrated the product distribution obtained from fluidized bed steam cracking of polyethylene is similar to that obtained from a tubular naphtha cracker [3]. Apart from fluidized bed reactors, other reactor configurations such as fixed bed and spouted bed reactors have also been proven effective for the thermochemical conversion of plastic materials [7,8].

Irrespective of the type of the reactor, thermochemical processes involve the conversion of the long-chained hydrocarbon molecules in plastic materials into simpler molecules such as light hydrocarbons, by breaking/cracking the carbon-carbon bonds [3–6]. The aim is to have a product distribution from thermochemical conversion of plastic materials that contains a large share of economically valuable hydrocarbons, such as ethylene, propylene, benzene, and toluene [3,4]. However, the cracking of hydrocarbon molecules during a thermochemical process also leads to the formation of undesirable products, such as polycyclic

* Corresponding author.
E-mail address: chahat@chalmers.se (C. Mandviwala).

https://doi.org/10.1016/j.jaap.2022.105603
Received 4 May 2022; Received in revised form 19 June 2022; Accepted 28 June 2022
Available online 30 June 2022

aromatic hydrocarbons (PAHs) and solid carbon deposits [4]. The production of PAHs and solid carbon makes the process economically unattractive because it lowers the direct production levels of the abovementioned valuable hydrocarbons [3]. The reaction mechanism underlying the formation of the first aromatic ring during hydrocarbon cracking is still a topic of debate. However, aromatization in a hydrocarbon-rich environment is usually attributed to the interactions between unstable free radicals and unsaturated hydrocarbon species formed in such a system [9,10].

Some successful efforts have been made to lower the formation of PAHs through steam reforming in a fluidized bed process [4,11]. For example, olivine has been shown to catalyze the steam reforming reactions of the degradation products, suppressing the formation of PAHs and solid carbon and enhancing the formation of syngas [4,11]. The generic steam reforming reaction is described by Eq. (1).

$$C_mH_{n(g)} + H_2O_{(g)} \rightarrow CO_{(g)} + H_{2(g)} \quad (1)$$

The reaction pathway described in Eq. (1) involves the interaction of water molecules with hydrocarbon species, leading to the transfer of oxygen atoms from the water molecules to the hydrocarbon species. Although steam reforming of the degradation products allows one to control the formation of PAHs, it does not guarantee enhanced formation of the valuable hydrocarbon species, but rather the formation of light syngas constituents. The increased formation of valuable hydrocarbon species and monomers, concomitant with suppression of PAH formation, can be ensured by hydrogenating the unsaturated hydrocarbon species that are formed by breaking the C-C bonds present in plastic materials. The hydrogenation reaction of 1-hexene, a common intermediate molecule formed during thermal conversion of polyethylene, is described in Eq. 2.

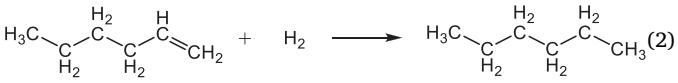

(2)

The thermochemical process that involves the cracking and hydrogenation of hydrocarbons is commonly referred to as the hydrocracking process [12]. The hydrocracking process involves the cracking of hydrocarbons followed by the hydrogenation of the cracked hydrocarbons by reactive hydrogen to produce stable and lighter hydrocarbons [12]. The hydrocracking process is commonly used to convert heavy petroleum products into lighter chemicals in the presence of a catalyst and a hydrogen atmosphere [12]. Hydrocracking facilitates the production of compounds that have higher hydrogen-to-carbon (H/C) ratios than the feedstock [12]. Although plastic materials like polyolefins have a high H/C ratio, the reduced formation of aromatics and solid carbon from the hydrocracking process makes it preferable over other processes, such as steam cracking and pyrolysis [6]. In addition, the presence of hydrogen enables the removal of heteroatoms such as chlorine, which may be present in plastic waste [6]. Because of the abovementioned reasons, hydrocracking of plastic materials, in particular polyolefins, has been studied extensively by many researchers [6].

Hydrocracking processes commonly use catalysts and operate at high pressure levels (up to 150 atm), which makes the hydrogen from the surroundings reactive to the hydrocarbon species [12–15]. In the absence of the catalytically active transfer sites and high-pressure environment, hydrogen is released as H_2 from the surroundings, such that it does not contribute to the hydrogenation reaction [12–15]. Therefore, the hydrogenation of the cracked hydrocarbons during hydrocracking depends on both the hydrogen donation capability of the surroundings and the hydrogen transfer capability of the catalyst [12–15].

An alternative to hydrocracking in hydrogen atmosphere is hydrocracking by hydrogen-donors, which has also been comprehensively studied [16–19]. The hydrogen released by the hydrogen donors hydrogenates the unsaturated hydrocarbons formed during the cracking reactions, as described in Eq. (2). The hydrogen donation capabilities of naphthenic hydrocarbons such as cyclohexane and decalin have been extensively described in the literature [18,19]. In addition, the hydrogen donation capability of water molecules in a supercritical steam environment has been studied in the context of upgrading heavy petroleum products [14,20–23]. Supercritical water has been shown to increase the H/C ratios of products, as compared to that of the feedstock, by transferring its hydrogen atoms to the hydrocarbon species. The transfer of hydrogen atoms occurs on the surface of a transition metal oxide catalyst and is linked to the water dissociation capability and the redox potential of the metal oxide catalyst [14,20–23]. Although hydrocracking by hydrogen donors (naphthenes, steam, etc.) is well-established in the petroleum industry, to the best of the authors' knowledge, such a process has not been studied for the conversion of plastic materials.

Furthermore, during the hydrocracking processes, the formation of solid carbon and feedstock impurities represents a serious problem. The catalytically active transfer sites undergo deactivation following the irreversible deposition of feedstock impurities and solid carbon on the catalyst surface [12]. As a consequence, a part of the catalyst inventory needs to be replaced with fresh catalyst to sustain the hydrocracking reactions. The sensitivity of the hydrocracking catalysts towards feedstock impurities represents an operational challenge for conventional hydrocracking processes that are dedicated to the conversion of feedstocks from plastic waste streams. Furthermore, treating heterogeneous plastic waste in slurry reactors, the most common type of reactor used for hydrocracking, is challenging. These challenges have hindered the development of hydrocracking processes for plastic waste at industrial scale.

Alternatively, a hydrocracking process dedicated to the conversion of plastic waste can be operated with a reactor configuration that is suitable for heterogeneous solid feedstocks and using a catalyst that is resistant to the feedstock impurities. In this sense, a fluidized bed reactor represents a suitable reactor configuration due to: (i) its ability to handle heterogeneous feedstocks; (ii) its high convective heat transfer rates; and (iii) enabling the possibility of introducing catalysts in the form of a bed material [3,4]. Natural ores such as silica sand, olivine and bauxite are less susceptible to the feedstock impurities compared to the conventional cracking catalysts [3,4]. However, the hydrocracking capability of a fluidized bed operated with natural ores remains unknown and unexplored, as of today.

This work aims to elucidate the hydrocracking capabilities of fluidized bed reactors operated with natural ores as the bed materials. In the present study, hydrocracking of polyethylene (PE) was investigated in a bubbling fluidized bed (BFB) reactor. The hydrogen donation capabilities of steam and the hydrogen transfer capability of the bed materials, the two critical parameters for hydrocracking, were examined in two steps. First, the capabilities of the different bed materials to generate H_2 via the water dissociation reaction were investigated in the absence of the polyethylene feedstock. Second, to determine the hydrogen donation capability of water, steam cracking was performed in parallel with the water dissociation reaction on the surfaces of two different bed materials, bauxite and olivine. Bauxite and olivine were chosen as the bed materials based on their abilities to undergo redox reactions and drive the water dissociation reaction [24]. As a reference experiment, steam cracking, in the absence of concurrent water dissociation reaction was performed.

2. Materials and method

2.1. Materials

The investigated bed materials were bauxite and olivine (500 g each). The properties of the bed materials used in this work are listed in Table 1.

The PE pellets used as the feedstock for this investigation which had a particle density of 945 kg/m^3 and pellet diameter of 2.5 mm, were

Table 1
Properties of the bed materials used in this work.

	Bauxite	Olivine
Al_2O_3	78%	0.46%
SiO_2	15%	41.7%
Fe_2O_3	1.3%	7.4%
MgO	0.2%	49.6%
Avg. particle size, d_p (mm)	0.29	0.31
Particle density (kg/m^3)	3000	3300
Minimum fluidization velocity, u_{mf} (m/s)	0.05	0.05

provided by Borealis AB. The PE pellets were taken from the same inventory as used in a previous study [25]. The proximate analysis of the PE pellets, along with the carbon and hydrogen contents, as previously reported by Mandviwala et al. [25], is presented in Table 2.

2.2. Experimental setup

Fig. 1 provides a schematic of the experimental setup used in this work. The bubbling fluidized bed reactor used in this work is a stainless-steel tube with an internal diameter of 88.9 mm and a height of 1305 mm. The reactor is placed in an electrically heated oven. The temperature along the height of the reactor is measured by the thermocouples placed inside the reactor. The fluidization gases are introduced from the bottom of the reactor through a gas distributor plate. The gases leaving the reactor are continuously sampled through one of the gas sampling probes h1 to h3. The sampled gas is divided into two split streams. One part of the sampled gas is analyzed in a SICK GMS 820 permanent gas analyzer after being cooled and dried in a gas conditioning system. The other part of the sampled gas is passed through a solid-phase extraction (SPE) amine and collected in a Tedlar gas bag. The condensable species are adsorbed on the SPE amine column, whereas the non-condensable species are collected in the gas bag. The procedure for quantification of all the sampled species is described in a previous study [25].

2.3. Water dissociation test

The water dissociation capabilities of bauxite and olivine, in their reduced form, were determined by performing a blank water dissociation test and quantifying the amounts of hydrogen released by the bed materials. The blank test was performed at a bed material temperature of 750 °C. The procedure for the blank water dissociation test is described in Table 3.

During the reduction stage, the bed materials were reduced with a mixture of CO and N_2 for 180 s. The iron oxide contents of the bed materials were reduced according to the following equation:

$$Fe_2O_{3(s)} + CO_{(g)} \rightarrow 2FeO_{(s)} + CO_{2(g)} \quad (3)$$

During the reduction stage, reduction of FeO to Fe is unexpected considering the reduction temperature of 750 °C [26]. Moreover, the reduction of the other metal oxides present in the bed materials (Al_2O_3, MgO, and SiO_2) by CO is also thermodynamically not feasible at 750 °C [26,27]. The reactor was then purged continuously with N_2 to create an inert atmosphere. After the reactor was rendered inert, the bed material was exposed to steam as one of the fluidization gases. Steam added to the reactor was converted into hydrogen by the bed material according to the following steam-iron reaction:

$$3FeO_{(s)} + H_2O_{(g)} \rightarrow Fe_3O_{4(s)} + H_{2(g)} \quad (4)$$

Since the metal oxides Al_2O_3, MgO, and SiO_2 remain in their fully oxidized state, they can be considered inactive toward the water dissociation reaction.

A fraction of the gases leaving the reactor during the blank test was sampled and analyzed for its composition (%vol) in the continuous gas analyzer. The known volume of N_2 (Table 3) was used to estimate the molar yield of hydrogen, according to the ideal gas law:

$$n_{H_2} = \frac{\%vol_{H_2}}{\%vol_{N_2}} \cdot n_{N_2} \quad (5)$$

where n_{H2} and n_{N2} represent the moles of N_2 and H_2, respectively, and $\%vol_{H2}$ and $\%vol_{N2}$ are the concentrations (%vol) of H_2 and N_2, respectively, in the gases leaving the reactor, as measured by the continuous gas analyzer.

Table 2
Properties of the PE pellets used in this work.

Proximate analysis	% wt.
Moisture content	0.00
Volatile matter	99.92
Fixed carbon	0.00
Ash content	0.08
Carbon & Hydrogen	
Carbon (C)	85.70
Hydrogen(H)	14.20

Source: [25].

2.4. Steam cracking (reference test without water dissociation)

PE pellets (2 g per batch) were fed directly onto the top of the fluidized bed. The weight of the feedstock represents a bed material to feedstock ratio of 250. A high bed material to feedstock ratio is used to avoid defluidization problem in the reactor. Steam cracking was performed at the bed material temperature of 750 °C. The temperature in the freeboard was maintained at 745 °C, at heights h2 and h3 (see Fig. 1). Each set was performed three times to ensure the repeatability of the experiments. The procedure for each set of steam cracking experiments is summarized in Table 4.

As described in Table 4, the fluidization gases were switched for each of the three stages of the experiment. During stage 1, the bed material was oxidized at the same reaction temperature of 750 °C. Oxidation of bed material was achieved by exposing the fluidized bed material to air, as described in Table 4. A fraction of the gases exiting the reactor was continuously analyzed for its O_2 concentration (%vol). Complete oxidation was assumed to have occurred when the O_2 concentration of the gases leaving the reactor matched the ambient O_2 concentration of 20.9% vol. The complete oxidation of the bed materials before the steam cracking stage ensured that there was no water dissociation reaction caused by the bed material during the steam cracking stage.

A known volume of helium (He) was used as one of fluidization gases during the steam cracking and carbon deposit combustion stages of each experiment. Fluidization with a known volume of He, together with the fluidization gases, facilitated the calculation of the total volume of gases produced during the steam cracking and carbon deposit combustion stages. The fluidization gas flow rate used throughout the experiment corresponded to a fluidization velocity that was 10–12 times the minimum fluidization velocity (u_{mf}) of the bed material used. The estimated minimum fluidization velocities of the two bed materials used in this work were 0.05 m/s.

During the steam cracking stage, the sampled gas was assayed for its H_2, CO, CO_2 and CH_4 concentrations (vol%) using the continuous gas analyzer. These concentrations were continuously monitored to assess the total time of steam cracking. The total time required for steam cracking was estimated as 120 s. For a detailed analysis of the other steam cracked species, a split steam of the sampled gas was passed through an SPE amine column. Gases exiting the SPE column were collected in a 0.5-L Tedlar gas bag. The gas bags with the collected gases were analyzed in the Agilent 490-micro-GC system. A summary of the gases measured by the micro-GC system is detailed in Table 5. Since the separation of individual C_3 and C_4 hydrocarbons was beyond the scope of the micro-GC system, the C_3 and C_4 hydrocarbons are collectively

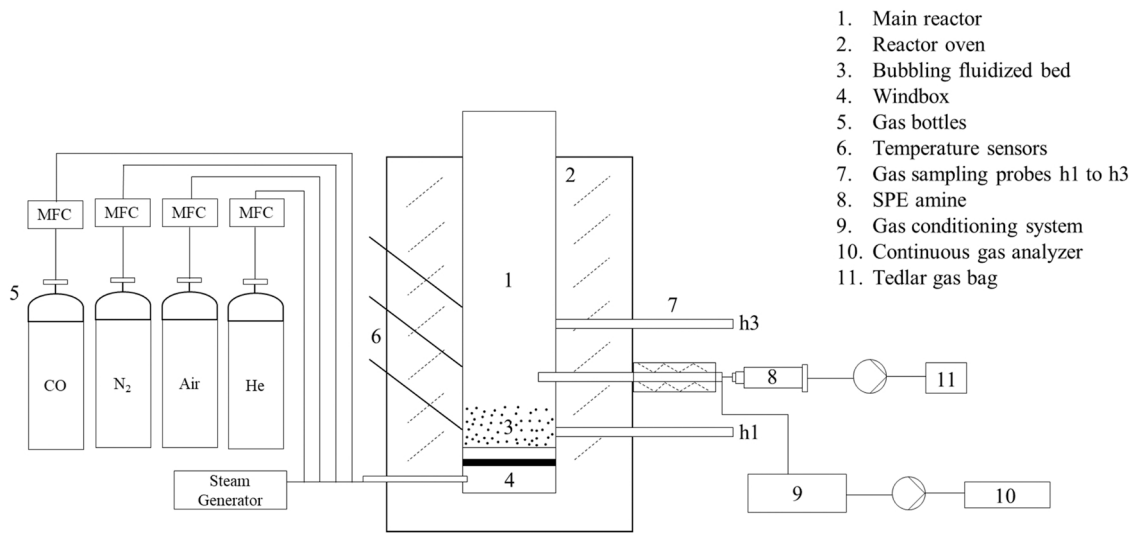

Fig. 1. Schematic of the experimental setup.
Source: [25].

Table 3
Experimental procedure for the blank water dissociation test.

Experimental stage	Fluidization gases (l_N/min)			Time
	N_2	Steam	CO	
Reduction	2.0	0.0	3.0	180 s
Inert	2.0	0.0	0.0	Until 0%vol CO
Hydrogen generation	2.0	4.0	0.0	Until 0%vol H_2

Table 4
Experimental procedure for steam cracking of PE.

Experimental stage	Fluidization gases (l_N/min)				Time
	Nitrogen	Steam	Air	Helium	
1. Oxidation of the bed material	0.0	0.0	5.0	0.00	Until 20.9% vol O_2
2. Steam cracking	2.0	4.0	0.0	0.05	120 s
3. Carbon deposit combustion	0.0	0.0	5.0	0.05	120 s

Table 5
Gases measured by the Agilent 490 micro-GC system.

Column	Gases
CP-Cox	He, H_2, Air, CO, CH_4
PoraPLOT U	CO_2, C_2H_4, C_2H_6. C_2H_2, C_3H_x
CP-WAX 52 CB	Benzene, Toluene
CP-Sil 5 CB	C_4H_x

represented as C_3H_x and C_4H_x in the following sections. The detection of aliphatic compounds with more than four carbon atoms was also beyond the scope of the analytic instruments used in this work.

The aromatic hydrocarbons were quantified with the BRUKER GC-FID system according to the solid-phase adsorption (SPA) method described by Israelsson et al. [28]. The redundant measurements of benzene and toluene on the CP-WAX column of the micro-GC system ensured that all of the benzene and toluene were captured and quantified by the SPA method.

Following steam cracking, solid carbon deposits remained in the reactor along with the bed material. The yield of solid carbon deposits in each bed material was determined by combusting it in presence of air and measuring the amounts of carbon oxides produced during the process. The fluidization gases were changed from nitrogen and steam to air, to allow combustion of the carbon deposits. The combustion gases were sampled for 120 s and collected in a separate 0.5-L Tedlar gas bag. The compositions of the collected combustion gases were measured using the micro-GC system.

2.5. Steam cracking with concurrent water dissociation

As mentioned in Section 1, the hydrogen donation capability of water molecules was determined by performing the steam cracking tests concurrently with the water dissociation reaction on the surface of the bed material. Concurrent water dissociation reaction was achieved by splitting the water molecules on the surface of the bed materials that contained iron oxide in a reduced form. The bed materials, prior to the steam cracking tests, were fluidized with a mixture of CO and N_2 in order to reduce the iron oxides present in the bed materials. The bed materials were fluidized with a CO/N_2 mixture until the concentration of CO_2 exiting the reactor reached 0% vol. The fluidization gases were then switched to N_2 for 2 min to purge the reactor and create an inert environment. Steam was added to the fluidized bed after the concentration of CO reached 0%vol.

The PE pellets were dropped directly on top of the reduced fluidized bed after steam was added to the reactor. That ensured the water dissociation reaction was initiated before the steam cracking reactions. The steam cracking products, with the hydrogen generated from the water dissociation reaction, were sampled for 120 s after the PE pellets were introduced into the reactor. The concentration profile of hydrogen obtained from the blank water dissociation test affirmed that the steam cracking and water dissociation reactions occurred simultaneously during the time window of 120 s. The procedure for sampling and analysis of the species produced during the steam cracking of PE with concurrent water dissociation was the same as that described in Section 2.3.

2.6. Data evaluation

The data evaluation procedure used in this work is adapted from a previous work [25]. The results reported in the following sections are the average values derived from the three repetitions of each experiment. The errors correspond to the standard deviations for the repetitions. The results were derived following the same sampling, analysis and evaluation procedures. As a result, the observed trends are expected to outweigh the systematic errors for all the data-points.

The He-tracing method was used to calculate the molar yields (mol/kg_{PE}) of the gaseous species collected in the Tedlar gas bags. The molar yields of all the measured gaseous species were calculated using Eq. (6).

$$n_i = \frac{c_i}{m_{PE}} \cdot \left(\frac{V_{He-tracing}}{C_{He}} \right) \cdot \frac{1}{V_m} \quad (6)$$

where n_i represents the molar yield, c_i is the concentration of gaseous species I, C_{He} and $V_{He\text{-}tracing}$ denote the concentration and volume of the tracer gas, respectively, m_{PE} is the weight of the PE pellets for each batch, and V_m is the volume of one mole of an ideal gas at 25 °C. The molar yield of each species was then converted to the respective carbon and hydrogen yield (%carbon and %hydrogen) depending on the carbon and hydrogen contents of the feedstock (see Table 2).

3. Results

3.1. Water dissociation

The concentration profile of the hydrogen gas, as logged by the continuous gas analyzer, produced during the blank water dissociation test is shown in Fig. 2. In Fig. 2, the time window of 25–145 s indicates the time during which the steam cracking of PE was performed in parallel to the water dissociation reaction after the blank test. The total amount of hydrogen (H_2) produced during the blank test were 0.013 mol and 0.019 mol for bauxite and olivine, respectively. The theoretical yield of H_2, calculated based on Eqs. (3) and (4), and the Fe_2O_3 content of bauxite and olivine (see Table 2), stood at 0.027 mol and 0.154 mol, respectively. The amounts of hydrogen produced during the indicated time window of 120 s corresponded to 0.012 mol and 0.017 mol for bauxite and olivine, respectively.

3.2. Carbon balance

Table 6 compares the product yields (%carbon and %hydrogen, by weight) derived from the steam cracking of PE at 750 °C, with and without concurrent water dissociation reaction on the surfaces of bauxite and olivine. Hereinafter, the reduced bed materials comprised of bauxite and olivine that have the capability to dissociate water are termed 'bauxite-H′' and 'olivine-H′', respectively. In their highest oxidation states, the bed materials are simply referred to as bauxite and olivine.

The results reported in Table 6 gives the global carbon balance for all the performed experiments. The error values represent the standard deviation for the three repetitions of each experiment, indicating the reproducibility of the experiments. The yields of carbon-containing species are calculated as %carbon (of the carbon content of the feedstock), and the yield of hydrogen gas (H_2) as %hydrogen (of the hydrogen content of the feedstock). The results obtained for the four experiments correspond to carbon balance closure values of 86%, 92%, 93% and 93%. The undetected carbon reported here is the difference between the total carbon in the feedstock and the amount of carbon measured in the products. The undetected carbon corresponds to aliphatic hydrocarbon species with more than four carbon atoms; measurements of these species were beyond the scope of the analytical methods used in this work.

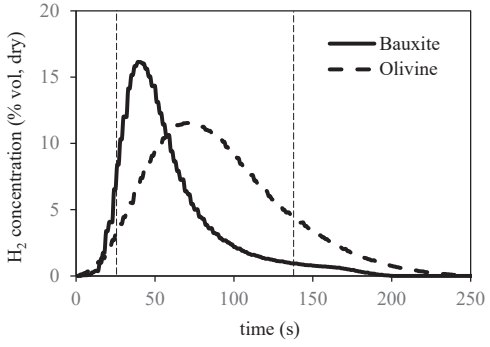

Fig. 2. Concentration profile of hydrogen produced during the blank water dissociation tests with the bed materials bauxite and olivine. The time window of 25–145 s indicates the time during which the steam cracking (parallel to water dissociation) tests were performed after the blank test.

Table 6
Distribution of the products obtained from the steam cracking of PE with and without concurrent water dissociation reaction. Carbon-containing species are reported in terms of their contribution (%) to the carbon balance, and H_2 is reported as its contribution (%) to the hydrogen balance. Values shown are 'mean' ± 'standard deviation'.

	Bauxite	Bauxite-H	Olivine	Olivine-H
Concurrent water dissociation	No	Yes	No	Yes
%wt. carbon				
C_2H_4	28.82 ±1.63	34.90 ±0.40	32.77 ±1.08	31.58 ±2.88
C_3H_x	10.25 ±0.19	11.17 ±1.09	12.90 ±0.90	12.59 ±1.10
C_4H_x	4.56 ±0.22	5.44 ±0.59	4.32 ±0.17	3.42 ±0.04
Total aromatics	20.67 ±0.53	16.82 ±0.64	21.47 ±0.65	21.45 ±0.49
Benzene	10.42 ±0.18	8.78 ±0.26	10.99 ±0.58	11.30 ±0.17
Toluene	3.30 ±0.08	2.71 ±0.02	3.41 ±0.09	3.45 ±0.02
Xylene	0.37 ±0.01	0.30 ±0.01	0.38 ±0.01	0.38 ±0.01
Styrene	1.60 ±0.08	1.16 ±0.05	1.65 ±0.01	1.46 ±0.06
Naphthalene	1.88 ±0.11	1.51 ±0.16	1.84 ±0.07	1.83 ±0.12
Others	3.09 ±0.53	2.36 ±0.16	3.19 ±0.08	3.02 ±0.12
Total paraffins	14.44 ±0.86	18.34 ±0.86	15.75 ±0.23	16.94 ±0.86
CH_4	10.98 ±0.72	13.59 ±0.78	11.87 ±0.06	12.52 ±0.64
C_2H_6	3.46 ±0.14	4.75 ±0.08	3.88 ±0.17	4.42 ±0.22
Total carbon oxides	4.90 ±0.13	4.22 ±0.03	4.63 ±0.45	5.61 ±0.15
CO	1.99 ±0.15	2.51 ±0.17	1.55 ±0.25	2.87 ±0.11
CO_2	2.91 ±0.02	1.71 ±0.20	3.08 ±0.20	2.74 ±0.04
Solid carbon deposits	2.64 ±0.26	1.08 ±0.09	0.82 ±0.16	1.31 ±0.08
Undetected[a]	13.72 ±2.33	8.03 ±1.94	7.14 ±3.19	7.10 ±4.32
%wt. hydrogen				
Hydrogen (H_2)	2.29 ±0.05	9.52 ±1.26	1.74 ±0.02	9.59 ±0.25

[a] 'Undetected' represents the difference between the total carbon in the feedstock and the amount of carbon in the measured products.

3.3. Product distribution

The results of this work (Table 6) are expressed as the share of carbon-containing species (%carbon) contributing to the carbon balance and the share of H_2 (%hydrogen) contributing to the hydrogen balance. The results provide a clear understanding of the carbon and hydrogen distributions among the products of steam cracking. Reporting the product yields as %weight of the feedstock can be ambiguous, specifically for carbon oxides, because the oxygen of carbon oxides can be derived from steam and the iron oxide content of the bed material and not from the feedstock itself. To facilitate an unbiased comparison with

the results reported in the literature, the results reported in Table 6 can be transformed to the %weight of the feedstock using the carbon and hydrogen contents (see Table 2) of the feedstock.

Methane, ethane, ethylene, C_3H_x and C_4H_x were the main gaseous products obtained from the steam cracking of PE with bauxite as the bed material. The aromatic hydrocarbons comprised mainly benzene, toluene, styrene and naphthalene. The combined yields of carbon atoms among the gaseous products were 74% and 63% for the steam cracking experiments with bauxite-H and bauxite, respectively. The higher yield of the carbon-containing gaseous products in the presence of the water dissociation reaction (74%) was due to remarkably higher yields of ethylene (34.90%) and methane (13.59%), as compared to the corresponding experiments conducted in the absence of the water dissociation reaction (28.82% and 10.98%, respectively). The total yields of aromatic hydrocarbons were 20.67% and 16.82% for bauxite and bauxite-H, respectively. Steam cracking in the presence of the water dissociation reaction produced significantly lower amounts of all the aromatic hydrocarbon species as compared to steam cracking without water dissociation. The total yield of carbon oxides was identical for bauxite (4.9%) and bauxite-H (4.22%). The yield of solid carbon deposits was slightly higher for bauxite (2.64%) than for bauxite-H (1.08%). The yields of hydrogen gas (H_2) were 2.29% and 9.52% (as %hydrogen of the feedstock) for bauxite and bauxite-H, respectively. The dramatic difference in yields of H_2 appeared to be attributed to the generation of H_2 from the water dissociation reaction in the presence of bauxite-H.

The main products obtained from steam cracking with olivine and olivine-H as the bed materials were methane, ethane, ethylene, C_3H_x, mono aromatics and naphthalene. Although a clear shift in product distribution was observed between the use of bauxite and bauxite-H as the bed materials, the product distributions obtained with the bed materials olivine and olivine-H were quite similar. The yields of gaseous products were 70% and 69% for olivine and olivine-H, respectively. Correspondingly, the total yields of aromatic hydrocarbons for olivine and olivine-H (21.47% and 21.45%, respectively) were identical. The yields of carbon oxides (4.63% and 5.61%) and solid carbon deposits (0.82% and 1.31%) were also near-identical for olivine and olivine-H, respectively. The only difference observed was in the yield of H_2 and that was because of H_2 generation from the water dissociation reaction in the presence of olivine-H.

The main products of PE steam cracking obtained with all four bed materials used in this work are comparable to those obtained by Jung and colleagues for fluidized bed conversion of PE at 728 °C [29]. Methane, olefins and mono aromatics were also the main products obtained by Kaminsky from fluidized bed steam cracking of PE at 740 °C [5]. However, the overall product distributions obtained in this work differ slightly from the distributions obtained by Jung and coworkers [29] and Kaminsky [5]. The yields (wt%) of C_2, C_3 and C_4 olefins reported by Kaminsky were 25.4%, 9.0% and 3.1%, respectively [5]. Jung et al. reported yields (wt%) of 21.5%, 10.5% and 5.3% for C_2, C_3 and C_4 olefins, respectively [29]. The combined yields of mono aromatics obtained by Kaminsky and Jung et al. corresponded to 16.9 wt% and 14.5 wt%, respectively [5,29]. The product distributions obtained by Kaminsky and Jung et al. are comparable to that obtained with bauxite in the present work (see Table 6).

The features and operating conditions of the reactors are important factors for explaining the results obtained in the cracking of polyolefins. The product distributions obtained with bauxite-H, olivine, and olivine-H differ slightly form those reported in the literature. The differences can be attributed to the differences in the bed materials used by both Kaminsky and Jung et al. (silica sand) [5,29] and those used in this work (bauxite and olivine). The increased formation of light olefins, concomitant with suppression of PAH formation, can also be achieved in a reactor configuration which enables high heating rates and short residence times [30,31]. Artetxe et al. obtained 77 wt% yield of light olefins by rapid thermal cracking of the low-temperature pyrolysis products of PE in a secondary tubular reactor [30,32]. Milne et al. obtained a similar selectivity to olefins (75 wt%) in an internally circulating fluidized-bed reactor, operating with a residence time of 0.4 s [31].

3.4. Effect of the water dissociation reaction

The extent of the hydrocracking reactions is usually linked to increases in the hydrogen contents of the produced hydrocarbons [14,20–23]. From the results shown in Table 6, it is clear that the share of hydrogen among the products of steam cracking is considerably higher with parallel hydrogen generation in the presence of bauxite-H or olivine-H. This increase is evident for the yield of hydrogen as H_2. The extent to which hydrogen atoms are transferred to the hydrocarbon species can be determined by comparing the H/C ratios of the steam cracking products obtained with and without the hydrogen generation reaction. The H/C ratios of the products are expected to increase in the presence of hydrogen transfer reactions.

An overall hydrogen balance, which involves the quantification of all olefinic, paraffinic and naphthenic species (C_3H_x, C_4H_x, C_5H_x, etc.), is required to determine the actual H/C ratios of the products. The quantification of individual C_3H_x and C_4H_x species was beyond the scope of the analytical instruments used in the work. Nonetheless, a range of H/C ratios of the obtained products was estimated rather than an exact value. The same approach was used in a previous study to determine the extent of dehydrogenation during steam cracking of PE [25].

For the purpose of determining the maximum value of the range, C_3H_x and C_4H_x were assumed to be C_3H_8 and C_4H_{10}, respectively, whereas for calculating the minimum value of the range, they were assumed to be C_3H_4 and C_4H_6, respectively. The ranges of the H/C ratios of the products obtained from the four experiments performed in this work are shown in Fig. 3.

It is evident from Fig. 3 that the ranges of the H/C ratios of the products obtained with bauxite (1.77–1.98) and bauxite-H (1.95–2.17) are significant different. In contrast, the ranges of the H/C ratios for olivine (1.83–2.06) and olivine-H (1.82–2.04) are identical. The increase in the H/C ratio of the products with bauxite-H as the bed material gives an indication of hydrogenation of the steam cracking products in the presence of the water dissociation reaction. However, the water dissociation reaction in the presence of olivine-H had no influence on the hydrogenation of the produced free hydrocarbon species, leading to similar H/C ratios of the products as was the case with olivine. The hydrogen produced from the water dissociation reaction on the surface of olivine-H appeared to be released entirely as H_2.

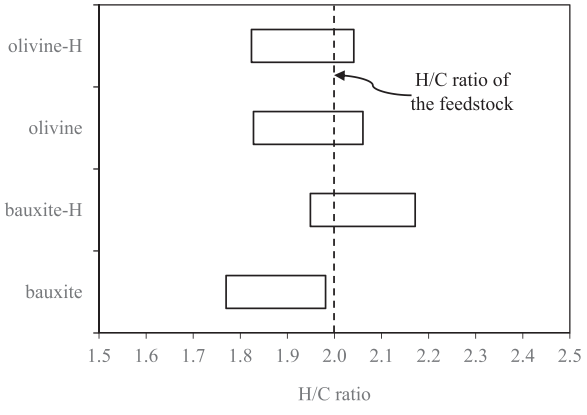

Fig. 3. Ranges of the H/C ratios of the products obtained from steam cracking of PE with the four bed materials.

4. Discussion

As mentioned in Section 1, the hydrocracking reactions are governed by two crucial process parameters: (1) the hydrogen donation capability of the surroundings; and (2) the hydrogen transfer capability of the catalyst. In the process used in this work, these parameters correspond to the hydrogen donation capability of water and the hydrogen transfer capability of the bed materials (bauxite and olivine), respectively.

From the results obtained in this work, it is clear that the hydrogen produced by the dissociation of water molecules on the surface of bauxite-H hydrogenates the hydrocarbon species produced during the steam cracking of PE. Compared to olivine olivine-H does not give a significant increase in the H/C ratios of the products. This discrepancy may be explained by differences in the abovementioned two parameters for the two materials investigated.

The hydrogen donation capability of water is related to the amount of hydrogen produced by the water dissociation reaction. The total amounts of hydrogen produced in the presence of bauxite-H and olivine-H, as estimated from the blank test, were 0.013 mol H_2 and 0.019 mol H_2, respectively. The amounts of hydrogen produced from the water dissociation reaction prove that the hydrogen donation capability of water is similar in the presence of bauxite-H or olivine-H. Despite the similar hydrogen donation capability of water, the hydrocracking phenomenon was observed only with bauxite-H, and not with olivine-H (see Fig. 3). Therefore, it is evident that olivine-H does not have a hydrogen transfer capability, resulting in H/C ratios of the products similar to those seen with olivine.

In the conventional hydrocracking processes, the hydrogen transfer capability of the catalyst is linked to the surface availability of the active sites and the characteristics of the catalyst support [12–15]. Although the bed materials used in this work do not resemble hydrocracking catalysts, some parallels can be drawn. The reduced iron present in bauxite-H and olivine-H that drives the water dissociation reaction can represent the active sites. That being said, the remainder of the bed material (SiO_2, Al_2O_3, and MgO), which remains inactive towards the water dissociation reaction, can be considered as the support for the active sites.

The surface availability of the active sites in bauxite-H and olivine-H can be compared by comparing the surface availability of iron oxide for both bed materials. The availability of iron oxide on the surface of natural olivine is known to be negligible from the previously reported literature [33,34]. The iron present as a silicate in natural olivine is known to migrate towards the surface, forming a hematite layer upon thermal treatments at temperatures above 850 °C [33,34]. The olivine bed material used in this work was never exposed to temperatures higher than 750 °C. Due to these reasons, the bed materials olivine and olivine-H are expected to have a negligible surface availability of iron as hematite. On the other hand, iron is present as individual particles of hematite in bauxite [35,36]. Therefore, the surface availability of iron is expected to be higher for bauxite, even though the total iron content of bauxite (1.3%wt.) was considerably lower than that of olivine (8%wt.), as reported in Table 1. Furthermore, the difference in the H/C ratio of the products obtained with bauxite and olivine (in their natural state) is also noteworthy. The range of H/C ratio obtained with bauxite (1.77–1.98) was slightly lower than that obtained with olivine (1.83–2.06). The presence of Fe_2O_3 on the surface of the bed material has been shown to lower the H/C ratio of the products obtained from the steam cracking of PE in a previous study [25]. That in addition to the previous arguments indicates that bauxite had a higher surface availability of iron compared to olivine.

The second parameter that affects the hydrogen transfer capability of the catalyst is the catalyst support. For the conventional hydrocracking catalysts, the active sites are supported by amorphous silica-alumina, or zeolite, or a combination of the two [12–15]. These catalyst supports are ideally porous materials that offer large surface area for the catalytic reactions [12–15]. In this sense, some of the properties of bauxite are comparable to those of a conventional hydrocracking catalyst support. Bauxite exhibits the constituent components of a hydrocracking catalyst support, i.e., aluminum oxide (Al_2O_3) and silicon dioxide (SiO_2). The bauxite used in this work had a combined Al_2O_3 and SiO_2 concentration of 93 wt% (see Table 1). In addition, bauxite is known to have porosity similar to that of hydrocracking catalyst supports [35,36]. Owing to these similarities, bauxite has also been used to prepare high-efficiency hydrocracking catalyst supports [35,36]. In contrast, the properties of olivine do not correspond to the properties of a hydrocracking catalyst support. Olivine, being a magnesium silicate, is known to contain negligible concentrations of free Al_2O_3 and SiO_2 [33,34].

It is clear from the above discussion that water dissociation (by the active sites) in a fluidized bed steam cracking process has the potential to hydrogenate the produced hydrocarbon species. The use of the bed materials (bauxite and olivine) with different properties revealed that the hydrocracking potential of a fluidized bed depends on the hydrogen transfer capability of the bed material. However, the influences of the bed material properties, such as the chemical composition, porosity, and the surface density of the active sites, on the hydrogen transfer potential of the bed material remain to be elucidated, and this is beyond the scope of the present work.

The fluidized bed hydrocracking process described in this work requires a cyclic process wherein the active sites of the bed material are exposed to a continuous cycle of reduction and oxidation. That is because the active sites once they are oxidized by the steam can no longer sustain the water dissociation reaction. Thus, continuous reduction of the active sites is required to sustain the water dissociation reaction. In this context, a dual fluidized bed (DFB) reactor configuration can be employed to create these conditions. A DFB system in which the bed material is reduced before it enters the hydrocracker is described in Fig. 4. The reduction agents used in such a system can be, for instance, methane, carbon monoxide, or hydrogen, which are obtained as the products of steam cracking. Such a configuration, when sealed thoroughly with non-mechanical valves called loop seals, will prevent the exchanges of gases between the three reactors [37]. That enables a continuous water dissociation reaction in the hydrocracker, thereby sustaining the hydrogen donation capability of the water.

A DFB system also has an advantage over standalone fluidized bed systems in that it can continuously remove the solid carbon deposits formed on the bed material through oxidation within the secondary fluidized bed (combustor). Steam cracking of plastic materials in fluidized beds has shown a significant formation of solid carbon deposits on the bed material compared to their fixed carbon content [4]. In addition, the presence of impurities (e.g., paper and cardboard) in the plastic waste streams will also lead to the formation of solid carbon deposits

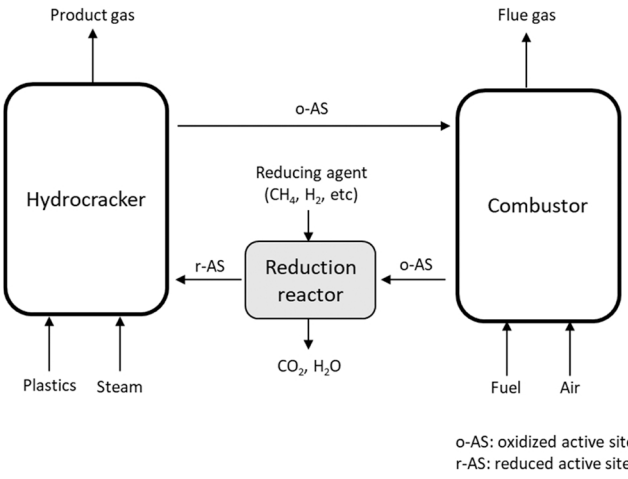

Fig. 4. Schematic of a DFB steam cracker that enables the continuous introduction into the hydrocracker of bed material that contains reduced active sites.

during the steam cracking process. In fluidized beds, the formation of carbon deposits on the bed material leads to the loss of the fluid phase and the heat transfer capacity of the fluidized bed [38]. Besides the removal of the carbon deposits, a DFB system has another advantage over a standalone fluidized bed in that the heat required for steam cracking can be conveniently transferred from the combustor to the steam cracker by the means of the bed material.

5. Conclusions

Hydrocracking of PE using hydrogenation by steam in a fluidized bed process was investigated in this work. The water dissociation reaction was used to generate the hydrogen for the hydrogenation step that is required for hydrocracking. The use of bauxite and olivine, in their reduced form, as the bed materials facilitated the water dissociation reaction. It is shown that the conversion of PE in the presence of reduced bauxite gives a product distribution with a higher range of H/C ratios, as compared to using bauxite in its highest oxidation state. The range of H/C ratios increased from 1.77-1.98 (for oxidized bauxite) to 1.94–2.16 (for reduced bauxite). Similar experiments performed with olivine and reduced olivine did not show a significant difference in the H/C ratios of the products. Despite the similar hydrogen donation capabilities displayed by water in the presence of reduced bauxite and olivine, hydrocracking of PE was observed exclusively on the surface of reduced bauxite. The main conclusion here is that hydrocracking through hydrogenation by steam is achievable in fluidized beds that are operated with natural ores as the bed materials, under the conditions that: (1) the bed material has the ability to drive the water dissociation reaction when it is in contact with the hydrocarbon feedstock; and (2) the bed material has the ability to transfer the generated hydrogen to the hydrocarbon species.

CRediT authorship contribution statement

Chahat Mandviwala: Conceptualization, Methodology, Investigation, Data curation, Writing-Original Draft. **Teresa Vilches Berdugo:** Investigation, Writing-Review & Editing, Supervision. **Martin Seemann**: Conceptualization, Supervision, Writing-Review & Editing, Project administration. **Judith González-Arias:** Methodology & Investigation. **Henrik Thunman:** Conceptualization, Writing-Review & Editing, Funding acquisition.

Declaration of Competing Interest

The authors declare that they have no known competing financial interests or personal relationships that could have appeared to influence the work reported in this paper.

Acknowledgments

This work was financially supported by Borealis AB, Sweden (Project number: 49514-1), the Swedish Gasification Center (SFC), Sweden and the Swedish Energy Agency, Sweden. The authors thank Jessica Bohwalli, Johannes Öhlin and Rustan Hvitt for technical support during the experiments.

References

[1] M. Rabnawaz, I. Wyman, R. Auras, S. Cheng, A roadmap towards green packaging: the current status and future outlook for polyesters in the packaging industry, Green Chem. 19 (2017), https://doi.org/10.1039/c7gc02521a.
[2] Organisation for Economic Co-operation and Development (OECD), Plastic Waste in 2019, OECD Environment Statistics (database), 2019. https://doi.org/https://doi.org/10.1787/a92f5ea3-en.
[3] H. Thunman, T. Berdugo Vilches, M. Seemann, J. Maric, I.C. Vela, S. Pissot, H.N. T. Nguyen, Circular use of plastics-transformation of existing petrochemical clusters into thermochemical recycling plants with 100% plastics recovery, Sustain. Mater. Technol. 22 (2019), https://doi.org/10.1016/j.susmat.2019.e00124.
[4] V. Wilk, H. Hofbauer, Conversion of mixed plastic wastes in a dual fluidized bed steam gasifier, Fuel 107 (2013), https://doi.org/10.1016/j.fuel.2013.01.068.
[5] W. Kaminsky, Chemical recycling of plastics by fluidized bed pyrolysis, Fuel Commun. 8 (2021), https://doi.org/10.1016/j.jfueco.2021.100023.
[6] D. Munir, M.F. Irfan, M.R. Usman, Hydrocracking of virgin and waste plastics: a detailed review, Renew. Sustain. Energy Rev. 90 (2018), https://doi.org/10.1016/j.rser.2018.03.034.
[7] S.M. Al-Salem, Thermal pyrolysis of high density polyethylene (HDPE) in a novel fixed bed reactor system for the production of high value gasoline range hydrocarbons (HC), Process Saf. Environ. Prot. 127 (2019), https://doi.org/10.1016/j.psep.2019.05.008.
[8] G. Elordi, M. Olazar, P. Castaño, M. Artetxe, J. Bilbao, Polyethylene cracking on a spent FCC catalyst in a conical spouted bed, Ind. Eng. Chem. Res. 51 (2012), https://doi.org/10.1021/ie3018274.
[9] R. Bounaceur, V. Warth, P.M. Marquaire, G. Scacchi, F. Dominé, D. Dessort, B. Pradier, O. Brevart, Modeling of hydrocarbons pyrolysis at low temperature. Automatic generation of free radicals mechanisms, J. Anal. Appl. Pyrolysis 64 (2002), https://doi.org/10.1016/S0165-2370(01)00173-5.
[10] J.F. Mastral, C. Berrueco, J. Ceamanos, Theoretical prediction of product distribution of the pyrolysis of high density polyethylene, J. Anal. Appl. Pyrolysis 80 (2007), https://doi.org/10.1016/j.jaap.2006.07.009.
[11] M.L. Mastellone, U. Arena, Olivine as a tar removal catalyst during fluidized bed gasification of plastic waste, AIChE J. 54 (2008), https://doi.org/10.1002/aic.11497.
[12] R. Saab, K. Polychronopoulou, L. Zheng, S. Kumar, A. Schiffer, Synthesis and performance evaluation of hydrocracking catalysts: a review, J. Ind. Eng. Chem. 89 (2020), https://doi.org/10.1016/j.jiec.2020.06.022.
[13] G. Alfke, W.W. Irion, O.S. Neuwirth, Oil Refining, in: Ullmann's Encyclopedia of Industrial Chemistry, 2007. https://doi.org/10.1002/14356007.a18_051.pub2.
[14] M. Hosseinpour, S. Fatemi, S.J. Ahmadi, Deuterium tracing study of unsaturated aliphatics hydrogenation by supercritical water in upgrading heavy oil. Part II: Hydrogen donating capacity of water in the presence of iron(III) oxide nanocatalyst, J. Supercrit. Fluids 110 (2016), https://doi.org/10.1016/j.supflu.2015.12.014.
[15] S. Funai, E. Fumoto, T. Tago, T. Masuda, Recovery of useful lighter fuels from petroleum residual oil by oxidative cracking with steam using iron oxide catalyst, Chem. Eng. Sci. 65 (2010), https://doi.org/10.1016/j.ces.2009.03.028.
[16] A. Matuszewska, A. Hańderek, K. Biernat, P. Bukrejewski, Thermolytic conversion of waste polyolefins into fuels fraction with the use of reactive distillation and hydrogenation with the syngas under atmospheric pressure, Energy Fuels 33 (2019), https://doi.org/10.1021/acs.energyfuels.8b03664.
[17] Z. Zhang, H. Chen, C. Wang, K. Chen, X. Lu, P. Ouyang, J. Fu, Efficient and stable Cu-Ni/ZrO2 catalysts for in situ hydrogenation and deoxygenation of oleic acid into heptadecane using methanol as a hydrogen donor, Fuel 230 (2018), https://doi.org/10.1016/j.fuel.2018.05.018.
[18] A. Hart, C. Lewis, T. White, M. Greaves, J. Wood, Effect of cyclohexane as hydrogen-donor in ultradispersed catalytic upgrading of heavy oil, Fuel Process. Technol. 138 (2015), https://doi.org/10.1016/j.fuproc.2015.07.016.
[19] L.O. Alemán-Vázquez, J.L. Cano-Domínguez, J.L. García-Gutiérrez, Effect of tetralin, decalin and naphthalene as hydrogen donors in the upgrading of heavy oils, Procedia Eng. (2012), https://doi.org/10.1016/j.proeng.2012.07.445.
[20] T. Sato, T. Sumita, N. Itoh, Effect of CO addition on upgrading bitumen in supercritical water, J. Supercrit. Fluids 104 (2015), https://doi.org/10.1016/j.supflu.2015.06.004.
[21] M. Hosseinpour, S. Fatemi, S.J. Ahmadi, Catalytic cracking of petroleum vacuum residue in supercritical water media: impact of α-Fe2O3 in the form of free nanoparticles and silica-supported granules, Fuel 159 (2015), https://doi.org/10.1016/j.fuel.2015.06.086.
[22] O.N. Fedyaeva, A.A. Vostrikov, Hydrogenation of bitumen in situ in supercritical water flow with and without addition of zinc and aluminum, J. Supercrit. Fluids 72 (2012), https://doi.org/10.1016/j.supflu.2012.08.018.
[23] M. Hosseinpour, S.J. Ahmadi, S. Fatemi, Deuterium tracing study of unsaturated aliphatics hydrogenation by supercritical water in upgrading heavy oil. Part I: Non-catalytic cracking, J. Supercrit. Fluids 107 (2016), https://doi.org/10.1016/j.supflu.2015.08.004.
[24] M. Luo, Y. Yi, S. Wang, Z. Wang, M. Du, J. Pan, Q. Wang, Review of hydrogen production using chemical-looping technology, Renew. Sustain. Energy Rev. 81 (2018), https://doi.org/10.1016/j.rser.2017.07.007.
[25] C. Mandviwala, T. Berdugo Vilches, M. Seemann, R. Faust, H. Thunman, Thermochemical conversion of polyethylene in a fluidized bed: impact of transition metal-induced oxygen transport on product distribution, J. Anal. Appl. Pyrolysis 163 (2022), 105476, https://doi.org/10.1016/j.jaap.2022.105476.
[26] M. Halmann, A. Frei, A. Steinfeld, Vacuum carbothermic reduction of Al2O3, BeO, MgO-CaO, TiO2, ZrO2, HfO2+ZrO2, SiO 2, SiO2+Fe2O3, and GeO2 to the metals. a thermodynamic study, Miner. Process. Extr. Metall. Rev. 32 (2011), https://doi.org/10.1080/08827508.2010.530723.
[27] L. Rongti, P. Wei, M. Sano, Kinetics and mechanism of carbothermic reduction of magnesia, Metall. Mater. Trans. B Process. Metall. Mater. Process. Sci. 34 (2003), https://doi.org/10.1007/s11663-003-0069-y.
[28] M. Israelsson, M. Seemann, H. Thunman, Assessment of the solid-phase adsorption method for sampling biomass-derived tar in industrial environments, Energy Fuels 27 (2013), https://doi.org/10.1021/ef401893j.
[29] S.H. Jung, M.H. Cho, B.S. Kang, J.S. Kim, Pyrolysis of a fraction of waste polypropylene and polyethylene for the recovery of BTX aromatics using a fluidized bed reactor, Fuel Process. Technol. 91 (2010), https://doi.org/10.1016/j.fuproc.2009.10.009.

[30] M. Artetxe, G. Lopez, G. Elordi, M. Amutio, J. Bilbao, M. Olazar, Production of light olefins from polyethylene in a two-step process: pyrolysis in a conical spouted bed and downstream high-temperature thermal cracking, Ind. Eng. Chem. Res. 51 (2012), https://doi.org/10.1021/ie300178e.
[31] B.J. Milne, L.A. Behie, F. Berruti, Recycling of waste plastics by ultrapyrolysis using an internally circulating fluidized bed reactor, J. Anal. Appl. Pyrolysis 51 (1999), https://doi.org/10.1016/S0165-2370(99)00014-5.
[32] M. della Zassa, M. Favero, P. Canu, Two-steps selective thermal depolymerization of polyethylene. 1: Feasibility and effect of devolatilization heating policy, J. Anal. Appl. Pyrolysis 87 (2010), https://doi.org/10.1016/j.jaap.2010.01.003.
[33] R. Faust, T. Berdugo Vilches, P. Malmberg, M. Seemann, P. Knutsson, Comparison of ash layer formation mechanisms on Si-containing bed material during dual fluidized bed gasification of woody biomass, Energy Fuels 34 (2020), https://doi.org/10.1021/acs.energyfuels.0c00509.
[34] L. Devi, M. Craje, P. Thüne, K.J. Ptasinski, F.J.J.G. Janssen, Olivine as tar removal catalyst for biomass gasifiers: catalyst characterization, Appl. Catal. A Gen. 294 (2005), https://doi.org/10.1016/j.apcata.2005.07.044.
[35] Y. Yue, J. Li, P. Dong, T. Wang, L. Jiang, P. Yuan, H. Zhu, Z. Bai, X. Bao, From cheap natural bauxite to high-efficient slurry-phase hydrocracking catalyst for high temperature coal tar: a simple hydrothermal modification, Fuel Process. Technol. 175 (2018), https://doi.org/10.1016/j.fuproc.2018.03.006.
[36] Y. Yue, P. Niu, L. Jiang, Y. Cao, X. Bao, Acid-modified natural bauxite mineral as a cost-effective and high-efficient catalyst support for slurry-phase hydrocracking of high-temperature coal tar, Energy Fuels 30 (2016), https://doi.org/10.1021/acs.energyfuels.6b01869.
[37] M. Stollhof, S. Penthor, K. Mayer, H. Hofbauer, Influence of the loop seal fluidization on the operation of a fluidized bed reactor system, Powder Technol. 352 (2019), https://doi.org/10.1016/j.powtec.2019.04.081.
[38] B.H. Davis, Fischer-Tropsch synthesis: relationship between iron catalyst composition and process variables, Catal. Today (2003), https://doi.org/10.1016/S0920-5861(03)00304-3.